

PFC/JA-84-33

Observation and Analysis of Maser Activity
in a Tokamak Plasma

R. F. Gandy, I. H. Hutchinson and D. H. Yates

Plasma Fusion Center
Massachusetts Institute of Technology
Cambridge, MA 02139

September, 1984

This work was supported by the U.S. Department of Energy Contract No. DE-AC02-78ET51013. Reproduction, translation, publication, use and disposal, in whole or in part by or for the United States government is permitted.

By acceptance of this article, the publisher and/or recipient acknowledges the U.S. Government's right to retain a non-exclusive, royalty-free license in and to any copyright covering this paper.

Observation and Analysis of Maser Activity in a Tokamak Plasma

R. F. Gandy*, I. H. Hutchinson and D. H. Yates

Plasma Fusion Center
Massachusetts Institute of Technology
Cambridge, MA 02139

Abstract

High resolution spectral measurements of electron plasma frequency emission from Alcator C tokamak reveal a level of coherence indicative of maser activity ($\Delta\omega/\omega=6 \times 10^{-6}$). A full-wave theoretical analysis yields the complete mode structure of the electromagnetic fields as well as the dispersion relation. This analysis shows that for wave frequencies near the central plasma frequency the waves are highly localized and thereby the plasma forms a high-Q cavity for these waves.

*Present Address: Physics Department Auburn University

Extremely intense radiation indicative of collective non-thermal emission processes is observed in a variety of laboratory and astrophysical plasmas [1] and its detailed understanding remains a key area of plasma physics.

In toroidal plasma experiments such as Tokamaks, emission is often observed near the electron plasma frequency [2-5]. The emission is of at least two types: quiescent, above the central plasma frequency, which has been interpreted [6-7] as due to spontaneous Cerenkov emission into the slow extraordinary mode; and fluctuating, which is the subject of the present study. Our results lead us to the clear inference that this fluctuating or 'bursting' emission is due to coherent maser action, in which the plasma itself acts as both the high Q cavity and the gain medium. In this Letter, we present high resolution spectral measurements of the fluctuating ω_{pe} emission from the Alcator C tokamak, which reveal the highly coherent nature of the emission. We have carried out a theoretical linear, electromagnetic analysis of the wave properties for monotonically decreasing electron density and finite magnetic field. The results of the calculations indicate that centrally localized wave-fields exist. This central trapping of the wave forms the basis of the maser action experimentally observed.

Previous measurements [3,4] revealed that the fluctuating emission from Alcator occurred at a frequency within 5% of the central plasma frequency (ω_{pe0}) and that the line-width of the spectral feature was narrow but unresolved ($\Delta\omega/\omega \lesssim 10^{-3}$). The bursting ω_{pe} emission is commonly observed during the early portion of the plasma pulse and immediately after the shut down of Lower Hybrid current drive [8]. Other observations confirm that the emission is contingent upon the presence of a high parallel energy tail on the electron distribution (runaways) but the tail is not

sufficient. For example, bursts are never seen during current drive, even though a tail is present.

The radiation bursts have a very rapid rise time, approximately one microsecond. They typically last 5-10 microseconds. Estimates of the total emitted power in a burst are of order 100 Watts, though precise estimates of emitted power are impossible because of restricted viewing geometry present on Alcator C.

All the experimental data reported in this Letter was observed with a 61 GHz radiometer. After collection the signal is passed through a 61 GHz high-pass waveguide filter. This filter provides image rejection by attenuating the lower sideband produced in the microwave mixer. The local oscillator is a Gunn diode operating at 61 GHz. With the image rejection filter, a typical intermediate frequency (IF) frequency range of 400 to 1500 MHz corresponds uniquely to a microwave frequency range of 61.4 to 62.5 GHz. The IF signal is subsequently amplified and all spectral measurements are made through analysis of the IF signal.

In order to examine a relatively wide range of IF frequencies (approximately 300 MHz) at high resolution (13 MHz), a surface acoustic wave (SAW) dispersive delay line was used to make real-time spectral measurements of the fluctuating ω_{pe} emission. A similar method has been used previously to measure the spectral width of far-infrared laser pulses [9]. The SAW output approximates a Fourier transform for a certain range of input pulse widths. A gated 100 nsec input pulse width was used to lie in this range.

The results from the SAW system indicate a wide variety of spectral phenomena. Single-peak and multiple-peak structures are seen. Almost all individual features observed were unresolved with a FWHM of 13 MHz, the instrumental resolution. Analysis of the peak-to-peak frequency spacing of the multiple bursts revealed no apparent regularity. The conclusion to be drawn from the SAW system is that a burst is composed of one or more irregularly-spaced narrow spectral features. The observation that the individual features were generally unresolved led us to employ a higher resolution technique.

A two-mixer, direct sampling technique was used to achieve a spectral resolution of 200 kHz. The basic idea behind the technique is to convert the microwave frequency signal to low enough frequency such that direct sampling can be accomplished using a fast A/D converter (32 MHz sampling rate). This is done by taking a portion of the IF signal from the microwave mixer (435-447 MHz) and passing it through a second mixer operating with a local oscillator frequency of 435 MHz. Image rejection is ensured by appropriate use of high-pass filters. Therefore, after the second mixer, the microwave signal range 61.435-61.447 GHz has been transformed to DC-12 MHz and may be directly sampled. The A/D converter is typically clocked for 5 microseconds (approximate duration of a burst). The sampled data is Fourier transformed to obtain the power spectrum.

Spectral widths in the range 400-800 kHz are observed. One of the narrower features is shown in figure 1 (FWHM=420 kHz). Another interesting feature is a frequency shift during certain bursts. This shift can be seen on the time domain data (fig. 2a) and on the transformed spectrum (fig. 2b). These frequency shifts are possibly related to changes in

longitudinal mode number and will be discussed later.

The theoretical cavity mode structure for waves near ω_{pe} may be obtained from an analysis taking the plasma to have cylindrical symmetry, and using the cold plasma dielectric tensor. Taking the applied magnetic field to be purely axial ($\underline{B}_0 = \hat{z}B$) solutions to Maxwell's equations proportional to $\exp i(kz + m\theta - \omega t)$ are sought, satisfying appropriate boundary conditions. The equations can be reduced to two second order equations [10] for the perturbed fields E_z and B_z which are coupled by the plasma anisotropy and inhomogeneity. These may be solved numerically, but for the case of interest, in which $\omega/\Omega \ll 1$ ($\Omega \equiv eB/m$) and $c/\omega_p a \ll 1$ (where a is the plasma radius) an accurate analytic approximation is possible. In this case, the equations decouple to second order in these small parameters and the E_z -mode (TM-mode), which has frequency just below the central plasma frequency ω_{p0} , and which corresponds approximately to the slow ordinary (whistler) branch of the homogeneous plasma dispersion relation, exhibits centrally localized solutions, trapped near the density maximum. Because of this localization, one can express the density profile as the (parabolic) first two terms of its Taylor expansion: $\omega_{pe}^2 = \omega_{p0}^2 (1 - r^2/a^2)$ and take the boundary condition to be $E_z \rightarrow 0$ as $r \rightarrow \infty$. The cavity modes are unaffected by the precise plasma edge conditions.

The E_z equation then becomes [11]

$$\left[\frac{1}{r} \frac{d}{dr} r \frac{d}{dr} - \frac{m^2}{r^2} + \mu^2 (\lambda^2 - r^2) \right] E_z = 0$$

where

$$\mu^2 = \frac{\chi_0 \omega_{p0}^2}{a^2 c^2} \frac{(N^2 - 1)^2 - N^4/Y^2}{N^2 - 1}$$

$$\lambda^2 = \frac{a^2(X_0-1)}{X_0} - \frac{c^2 2m N^2}{\omega_{po}^2 Y(N^2-1)}$$

$X \equiv \omega_{pe}^2/\omega^2$, $Y = \Omega/\omega$, $N = kc/\omega$ and subscript zero indicates central value. The solutions of this equation are

$$E_z = L_n^m(\mu r^2) (\mu r^2)^{m/2} \exp(-\mu r^2/2)$$

where L_n^m is the associated Laguerre polynomial. The mode number n , which must be integral to satisfy the boundary condition at ∞ , is given by the equation

$$\lambda^2 \mu = 2(2n + m + 1),$$

which is the required dispersion relation linking ω and N for given m and n . It may be solved to give:

$$\omega = \left\{ \omega_{po} \left[1 - \frac{2(2n + m + 1)}{\omega_{po} a/c} \left[\frac{N^2-1}{(N^2-1)^2 - N^4/Y^2} \right]^{1/2} \left[1 - \frac{2mN^2}{(2n + m + 1)(N^2-1)^{3/2} Y \omega_{po} a/c} \right]^{-1/2} \right] \right\}^{1/2}$$

which shows that the eigenfrequency is slightly below the central plasma frequency.

In Figure 3, we show the wave mode structure of the three lowest order eigenmodes for plasma parameters typical of the Alcator C experiments, and parallel refractive index $N=1.3$. The modes are, as anticipated, highly localized near the axis, $r=0$; for slower waves, $N>1.3$, this localization is even more pronounced. This central trapping is essential for Masing to occur.

Thermal effects can be taken into account [11] in the real part of the frequency in the form of Bohm-Gross dispersion by multiplying the above mode frequency by $(1 + 3N^2v_t^2/c^2)^{1/2}$. The gain of the medium i.e. the imaginary part of the frequency, ω_i , depends on the details of the electron distribution function. 'Cerenkov' (Landau) gain arising from the wave particle resonance at $\omega = k_{\parallel} v$ requires a positive slope on the parallel distribution function and the growth rate is approximately the same as for a homogeneous plasma:

$$\omega_i = \frac{\pi}{2} \frac{c^2}{N^2} \frac{df}{dv_{\parallel}} \bigg|_{c/N} \cdot \omega_r$$

(with small corrections for the inhomogeneity [11]). The positive value of the df/dv_{\parallel} corresponds to the population inversion in the Maser. It is believed to arise from the pitch angle scattering of electrons by waves arising from the anomalous cyclotron resonance (Parail-Pogutse) instability [12-14] Therefore, one can think of these latter waves as being the 'pump' of the Maser.

The longitudinal group velocity, v_g , of the waves can be deduced from the previous formulae and enables a calculation of the longitudinal mode spacing $\Delta\omega$ of the cavity to be obtained, $\Delta\omega = v_g/R$, where R is the major radius (0.64m for Alcator C). If the multiplet structure of the figure 2 is interpreted as due to shifting between adjacent longitudinal mode numbers, the v_g equation allows us to deduce the parallel index of refraction, N, from the experimentally observed frequency shift. For the example presented in figure 2, a value of $N = 1.3$ is found, which corresponds to a resonant longitudinal electron energy of 300 keV.

The transverse mode spacing is much larger, typically ~ 400 MHz, and may explain the occasional occurrence of larger frequency shifts. The 'output coupling' mechanism of this Maser is still uncertain. The mode structures calculated indicate that the field at the plasma edge is quite negligible for typical parameters and toroidal effects are weak. Therefore, some form of scattering from unknown density perturbations must probably be invoked [15] to account for the observed free space radiation.

In summary, high resolution spectral measurements of fluctuating ω_{pe} emission from Alcator C demonstrate a highly coherent maser action. Analysis of wave structure in bounded plasma for appropriate parameters reveals centrally trapped plasma waves. This trapping explains how the plasma can naturally form the high-Q cavity required for masing and provides the quantitative relationship between the cavity wave frequency and the central plasma frequency.

This work was supported by U.S. Department of Energy contract

#DE-AC02-78ET51013.

References

- ¹See e.g. K. Papadopoulos and H. P. Freund, Space Sci. Rev. 24, 511 (1979).
- ²A. E. Costley and TFR Group, Phys. Rev. Lett. 38, 1477 (1977).
- ³I. H. Hutchinson and D. S. Komm, Nucl. Fusion 17, 1077 (1977).
- ⁴I. H. Hutchinson and S. E. Kissel, Phys. Fluids 23, 1698 (1980).
- ⁵I. H. Hutchinson and S. E. Kissel, Phys. Fluids 26, 310 (1983).
- ⁶H. P. Freund, L. C. Lee and C. S. Wu, Phys. Rev. Lett. 40, 1563 (1981).
- ⁷K. Swartz, I. H. Hutchinson and K. Molvig, Phys. Fluids 24, 1689 (1981).
- ⁸M. Porkolab et.al., Phys. Rev. Lett. 53, 450 (1984).
- ⁹H. R. Fetterman, et.al. Appl. Phys. Lett. 34, 123 (1979).
- ¹⁰e.g. W. P. Allis, S. J. Buchsbaum and A. Bers, "Waves in Anisotropic Plasmas", MIT, Cambridge, MA (1963).
- ¹¹I. H. Hutchinson and R. F. Gandy, to be published.
- ¹²v. V. Parail and O. P. Pogutse, Fiz. Plazmy 2, 228 (1976) [Sov. Plasma Phys. 2, 125 (1976)]
- ¹³C. S. Liu et.al., Phys. Rev. Lett. 39, 701 (1977).
- ¹⁴K. Molvig, M. S. Tekula and A. Bers, Phys. Rev. Lett. 38, 1404 (1977).
- ¹⁵I. H. Hutchinson, K. Molvig and S. Y. Yuen, Phys. Rev. Lett 38, 1404 (1977).

Figure Captions

- Fig. 1. Power spectrum of bursting ω_{pe} emission. The frequencies have been downconverted by 61.435 GHz. The feature centered at 10 MHz has a FWHM of 420 KHz.
- Fig. 2. (a) Raw data from direct-sampling method. Note shift to higher frequency as time increases; (b) power spectrum of data shown in 2(a). Triplet spectral feature is revealed.
- Fig. 3. Three lowest order solutions (m, n) to E_z eigenmode equation versus normalized plasma radius, for plasma parameters appropriate to the experimental results: $\Omega/\omega = 5$, $\omega_{pa}/c = 160$ and $N = 1.3$. Also shown is the assumed parabolic density profile.

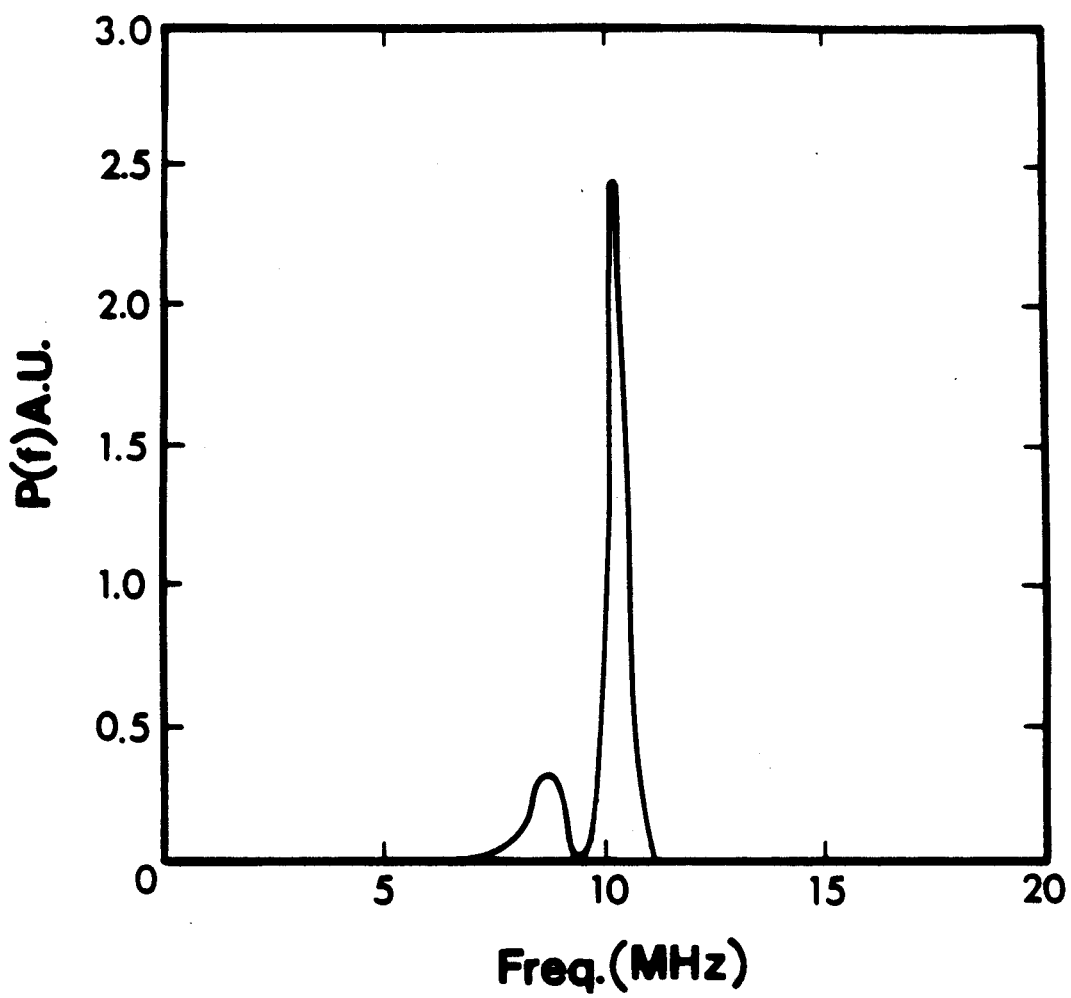


FIGURE 1

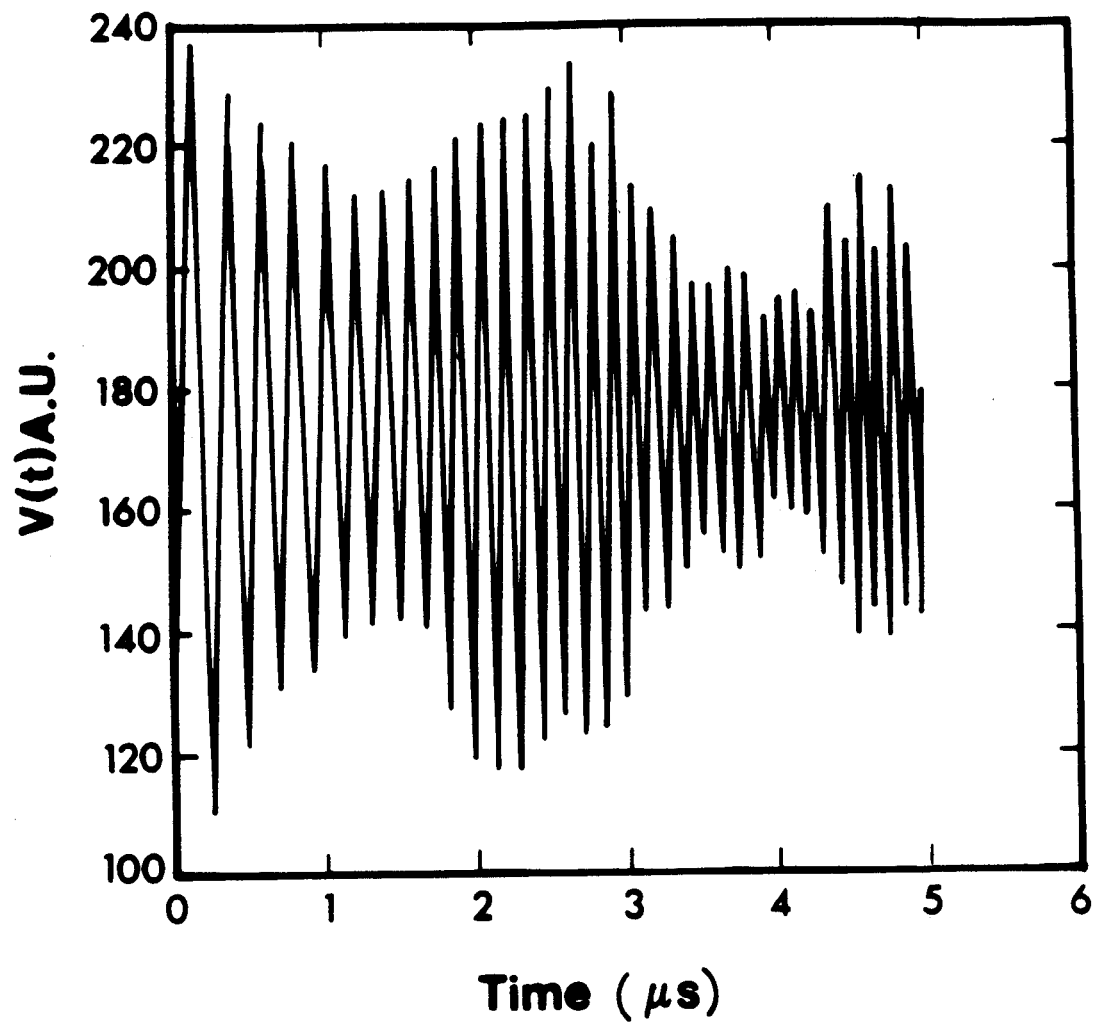


FIGURE 2a

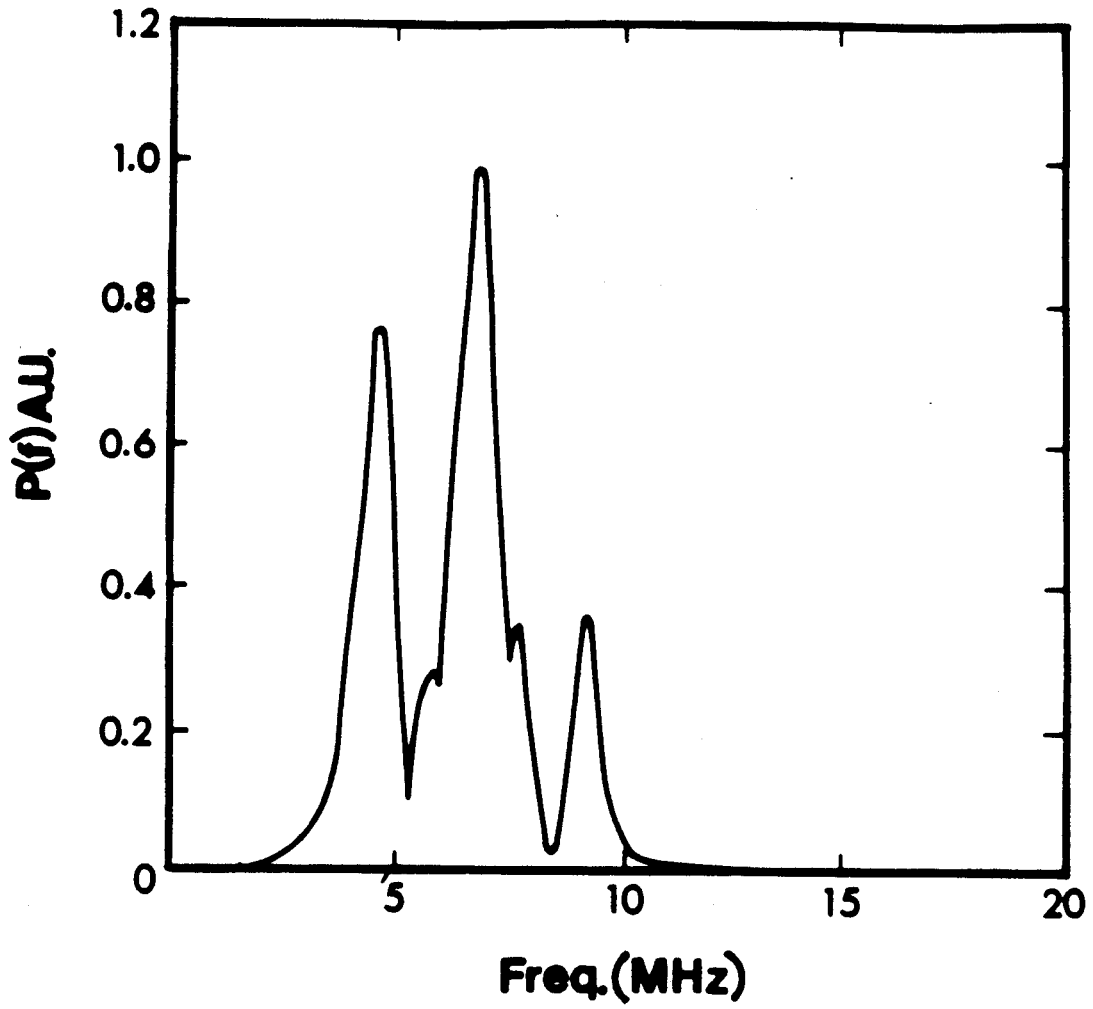


FIGURE 2b

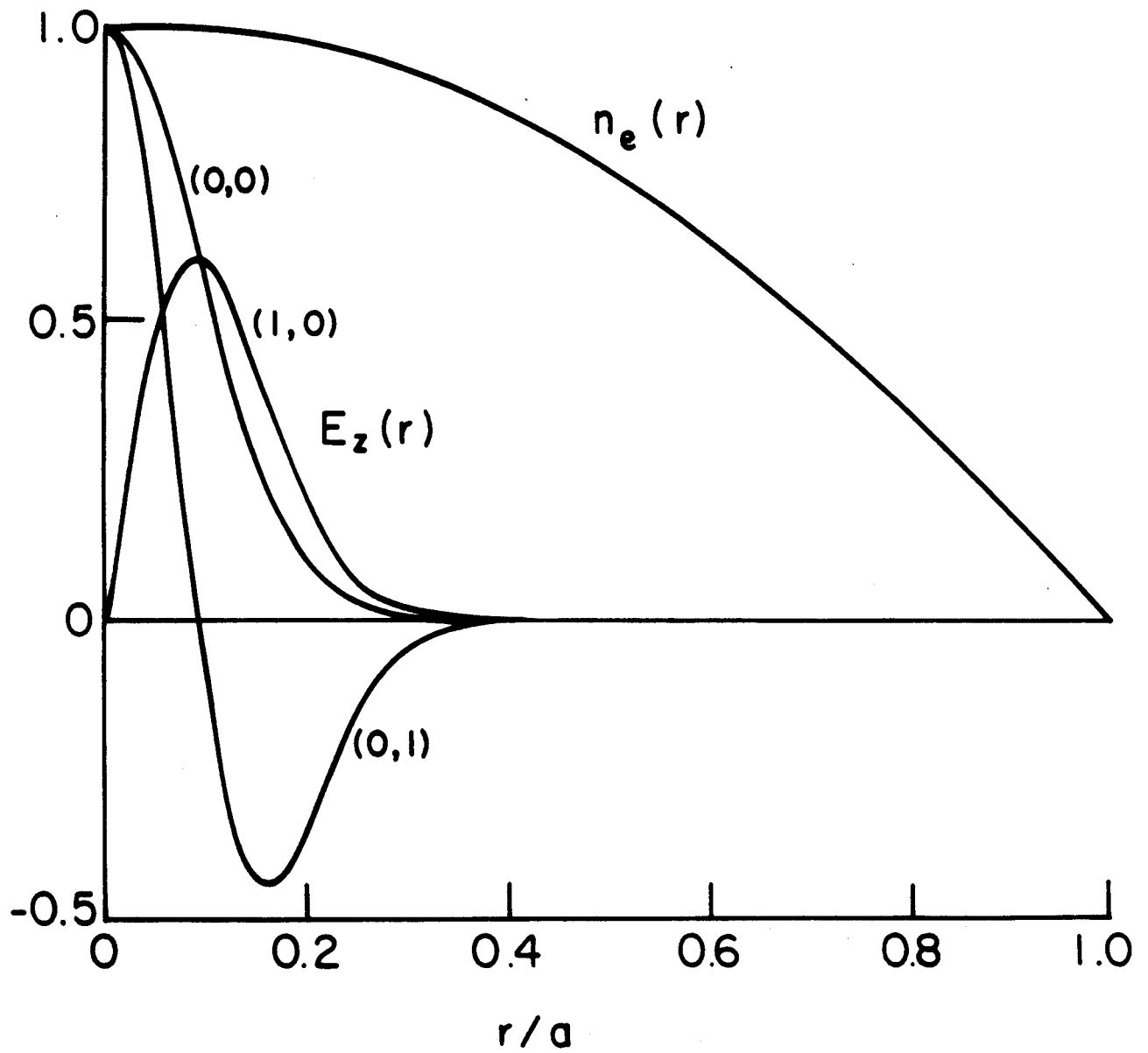


FIGURE 3